2018 7th IEEE International Conference on Biomedical
Robotics and Biomechatronics (Biorob)
Enschede, The Netherlands, August 26-29, 2018

A radar-based terrain mapping approach for stair detection towards enhanced prosthetic foot control

Bernhard Kleiner[1], Nils Ziegenspeck[1], Roman Stolyarov[2], Hugh Herr[2], Urs Schneider[1], Alexander Verl[3]

Abstract— **Current developments in ankle prosthetics are focusing on integrated actuators to fully control torques and angles. This enables terrain adaptive strategies e.g. for stairs and ramps. EMG and motion sensor input are state of the art approaches to classify different terrain or terrain changes, but these approaches have limited capabilities and detection accuracy. We present a novel approach for the detection of obstacles using a wearable Frequency-Modulated Continuous Wave (FMCW) radar integrated into a lower limb prosthetic device. With the continuous rotational motion of the tibia during the swing and stance phase, the radar scans the profile of the terrain in sagittal plane in front of the prosthesis. Gait phases are detected using a neural network classifiers based on inertial sensor data. Performance of the system is demonstrated in a single stair detection scenario.**

I. INTRODUCTION

Todays latest prosthetic ankles are adaptive devices which are partly capable of generating a natural gait pattern [1]. These devices are still limited due to sparse and unreliable real-time information about human intention with the surrounding terrain. In particular, interacting with stairs requires kinetic and kinematic adaptation very different from that required for level ground walking. Passing a single stair requires foot clearance during swing as well as additional torque and power delivery during stance.

A. Related work

Three sensory based strategies are predominantly used to provide information to ankle-foot prostheses: (1) The detection of users intention based on electromyography (EMG), (2) estimation of terrain using the ground reaction forces, and (3) prediction of terrain using inertial measurement units (IMU)[2]. EMG approaches have the advantage to estimate the intention of the user in advance [3], but the quality of the EMG signal tends to vary significantly with residual limb state (persperation, temperature) and constitution (soft tissue thickness, surface hair). Ground reaction force (GRF) in combination with IMU based inclination data are used in [4] to distinguish between ground, ramp ascent and ramp descent. The inclination of foot and shank is evaluated during stance and swing phase. Both are detected using a load cell and angle measurement. This method can provide control input after the interaction with the terrain and cases a delayed adaption of torque and joint angles. In [5] a method is presented to measure the terrain using a laser based 2D scanner mounted on a prosthesis. This approach showed the potential of terrain detection as an input for prosthesis control. As lasers cannot be hidden behind clothes, such a system would be rejected by most patients. Additionally, laser scanning modalities are weaker in outdoor conditions like direct sunlight, dust, fog and dark surfaces. In [6] a radar sensor is applied for potential stair detection in wheelchair and prosthesis applications. Radar signals can measure through non-conducting materials and are invariant to lighting condition and surface textures. Even though radar reflection signatures of objects are not deterministic and blurred, we developed a method to estimate stair height levels by radar scans [6][7].

[1]Fraunhofer Institute for Manufacturing Engineering and Automation IPA, Department of Biomechatronic Systems, Germany bernhard.kleiner@ipa.fraunhofer.de
[2]Massachusetts Institute of Technology, Center for Extreme Bionics, USA hherr@media.mit.edu
[3]University Stuttgart, Institute of Control Engineering of Tool Machines and Manufacturing Units ISW, Germany alexander.verl@isw.uni-stuttgart.de

II. TERRAIN DETECTION

A. Requirements for terrain detection

In this section basic requirements for an integrated stair detection system are analyzed:

- Detection of stairs before interaction
- Detection of stairs with a minimum height of 1 cm
- Invariance to sensor occlusion, lighting, humidity and surface texture

Regarding the first requirement, stair detection needs to occur with sufficient time for the prosthesis to react. The reaction time is defined by the prosthesis specific function e.g. (dorsal flexion, ankle torque adjustment). For example, BiOM ankle [8] can adjust its ankle torque from minimum to maximum within about 200 ms.

Regarding the second requirement, a study evaluated toe clearance for non-amputees over a long time period [9]. Especially elderly have significant low toe to ground distances. Even a door sill with a height of 1 cm can cause stumbling. Approximately 70 % of all above knee amputees still fall once per year which is mostly caused by stumbling over unrecognized obstacles. The prostheses might be covered by the patient with clothes. Furthermore, dust, humidity, and dirt can be present in outdoor scenarios, and surface texture in both indoor and outdoor application is not controllable. Thus, a sensor system is required to be invariant to those issues.

B. Significance of terrain detection

Previous studies on biological gait have shown that metrics of gait biomechanics can vary significantly not only across terrain types but also across varying geometries for the

978-1-5386-8183-1/18/$31.00 ©2018 IEEE

same terrain [10]. In particular, knee and ankle kinetics and kinematics can change significantly depending on the stair height, beginning with the stance phase prior to stair ascent or descent. Therefore, early detection of stairs with either a transfemoral or transtibial prosthesis (such as the BiOM) would allow for variation in power and torque delivery during stance, at levels informed by the detected stair height. In addition, different levels of ground clearance could be attained through swing phase dorsiflexion in response to the detected stair height, provided that the prosthesis is able to dorsiflex to the biologically appropriate angle for the given height. Similarly, detection of stair depth during descent tasks would enable modulation of late stance power delivery, knee and ankle angle at foot strike, and early stance damping. This cognition ability is not covered in the presented approach.

C. Terrain Mapping Approach

The prosthesis system is continuously moving during swing and stance phase. A dominant motion component is the translation and rotation in sagittal plane. The integrated distance measurement system pointing in walking direction continuously senses the structure in front of the prosthesis as shown in Fig. 1. Mapping of all measured distances needs a distance sensor and a motion measurement with respect to a global coordinate frame. In section III we introduce a measurement system consisting of a radar and an inertial measurement unit (IMU) to achieve these capabilities.

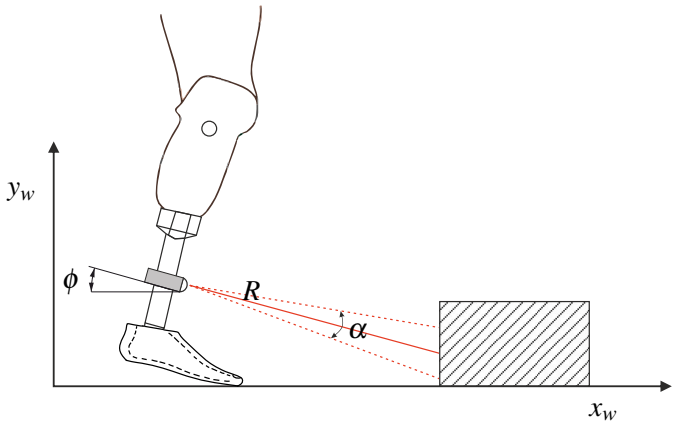

Fig. 1. Radar scanning approach during stance phase with ϕ angle of the radar system, R distance from the radar to an object and α the opening angle of the radar sensor.

III. MEASUREMENT SYSTEM

The measurement system consists of a Frequency Modulated Continuous-Wave (FMCW) radar for distance measurement and an IMU for trajectory estimation. Both sensors are attached to the tibia section as shown in Fig. 1. This setup is extended with two reference systems, an infrared motion capturing system from Vicon and a pressure insole from Tekscan. The setup was attached on test subjects wearing a BIOM prosthesis.

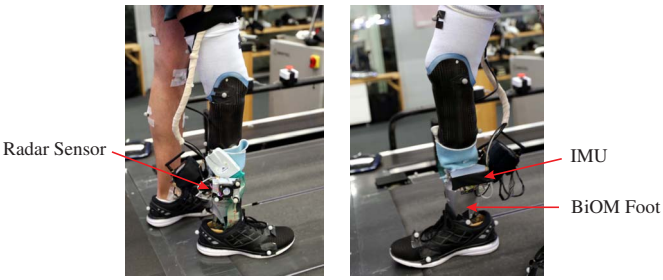

Fig. 2. Measurement setup on the patient

A. W-Band FMCW Radar sensor

Radar sensors are known to handle harsh outdoor conditions and are invariant to sunlight, dust, and terrain texture. Despite the fact that radar sensors are compared to optical sensors low resolution sensors for structure measurement, they can still function covered behind clothes and cosmetics. The sensor used during the experiment is a 94 GHz FMCW radar [11] with full control over all measurement parameters. The emitted signal modulation is a saw tooth chirp with a duration T_p and a repetition at 160 Hz. Each chirp is a linear increasing frequency signal with the bandwidth B. The received target echos have a frequency shift, corresponding to the velocity, and a time shift, corresponding to the distance. The received and transmitted signal are mixed down to the mid frequency f_z. With this, all echos result in a superposition of frequency signals f_z. To calculate distances, a fast Fourier transform (FFT) is applied to f_z. From (1), the range is calculated by:

$$R = \frac{cT_p f_z}{2B} \tag{1}$$

with c for speed of light, the chirp duration T_p, the mid frequency f_z and chirp bandwidth B. The radar has a limited range resolution δ_r to differentiate objects, which is inversely proportional to the bandwidth B of the chirp sequence.

$$\delta_r = \frac{c}{2B} \tag{2}$$

The resolution is set to 3.2 cm which is suitable for our application based on the bandwidth of 4.8 GHz. From (3), the maximum range R_{max} is the range resolution δ_r scaled by N_s, the number of samples per chirp.

$$R_{max} = \frac{cN_s}{2B} \tag{3}$$

The antenna design influences the detection capabilities. The used antenna is a Vivaldi antenna with a polymer lens to achieve an opening angle (-3 dB) of 11°. All relevant radar parameters are listed in Table I.

B. Inertial Measurement Unit

The inertial measurement unit consists of three orthogonal gyroscopes and accelerometers and is strapped orthogonal to the radar measurement direction, making an additional calibration for axis alignment unnecessary. The purpose of the inertial sensor is to estimate the trajectory of the radar sensor during the stance phase with an accuracy in the range

TABLE I

SPECIFIED PARAMETER OF THE 94 GHZ RADAR SENSOR

Radar Parameter	Specification
Center-Frequency	94 GHz
Bandwidth (B)	4,8 GHz
Chirp Duration (T_p)	220 µs
Chirp Modulation	Saw Tooth
Chirp Period	160 Hz
Antenna	Vivaldi Antenna
Maximum Distance (R_{max})	6.25 m
Samples per Chirp (N_s)	200
Opening Angle (α)	11°

of 1 cm. Therefore, the high end MEMS-IMU M-G364 from EPSON is considered which has been proven for hand held position estimation [12]. The relatively slow measurement range of $\pm$ 200 $^\circ s^{-1}$ and ± 3 g is adequate for stance phase dynamics.

C. Human Body and mm-Wave radar

Due to the use of the radar sensors closed to the human, it is necessary to consider the effects of radiation on living beings. The millimeter wave band (W-Band) ranges from 30 GHz to 300 GHz with an associated wavelength from 10 mm to 1 mm. Unlike ultraviolet and gamma radiation, W-Band radiation is non-ionizing. The main effect of radar is the heating of tissues such as eyes and skin due to absorption of the energy through the human body [13]. Emission limits are recommended by the International Commission on Non-Ionizing Radiation Protection [14], which are internationally recognized. The directional power density of the radar system at a distance R is calculated with (4) from the non-directional power density S_u and the antenna gain G. The maximum antenna gain of the used 94 GHz radar is 20 dBi, which corresponds to an antenna gain of $G = 100$. The output power of the radar chips is according to [11] $P_s = 2$ mW and was determined experimentally.

$$S_g = G \cdot S_u = G \cdot \frac{P_s}{4\pi R^2} \tag{4}$$

The shortest possible distance to the radiation source (antenna) is in front of the radar sensor with 1.5 cm . The polymer lens is placed after the antenna and there is no direct access to the Vivaldi antenna. The directed power density S_g at a distance of 1.5 cm is 7.07 mW/cm^2. It represents an extreme value during direct contact with the radar sensor and is still below the limits. However it is recommended to turn off the radar emission temporarily if complete occlusion is detected.

D. Experimental setup

The radar sensor and the inertial measurement unit are both mechanically fixed on the housing of the BiOM prosthesis as shown in Fig. 2. The radar is directed forward with a 10° tilt in sagittal plane at a height of 0.23 m. Vicon motion capture and a Tekscan pressure sole are used as a reference.

IV. PROSTHESIS MOTION ESTIMATION

Position and orientation estimation using inertial sensors is a widely studied topic [15]. Initialization errors, bias drift, and discretization errors lead to non observable estimation errors due to double integration of acceleration data. To compensate these errors, orientation angles can be estimated robustly with acceleration and gyro sensor data using e.g. a full observable Kalman filter. As mentioned in section II, the pose of the radar sensor is used only during the stance phase. Therefore, a model is proposed to calculate the motion of a point on the tibia section with respect to the inertial reference frame.

A. Trajectory estimation during stance phase

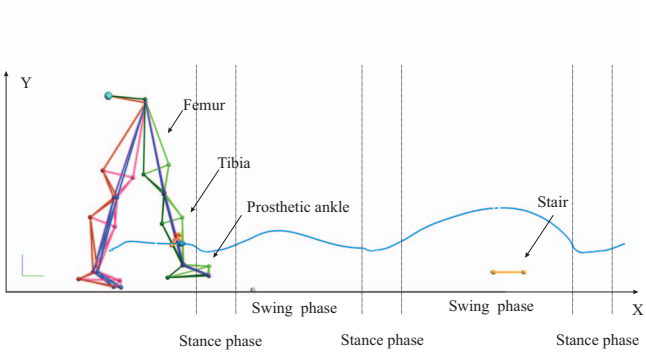

Fig. 3. Trajectory (blue) of the radar sensor mounted on the tibia measured by Vicon Motion Capturing System

A possibility for modeling the movement of the radar attached to the tibia section is the consideration of the human gait and the derivatives of models whose output quantities have better accuracy than the general system model. In Fig. 3, the motion trajectory of the radar is shown in sagittal plane. Similar shapes in stance phases are clearly recognizable. In [16] the roll-over movement of a prosthetic foot was investigated as a function of running speed. It has been proven that the rolling behavior of a prosthetic foot does not significantly change with respect to the walking speed. The corresponding rolling curve, also named roll-over shape, is the distance of a fixed point on the tibia to the current center of pressure on the prosthetic foot. According to this investigation, the motion of the fixed point of the tibia in respect to the starting point of the stance phase on the ground should not vary significantly. A model was developed to calculate the position of a fixed point on the tibia in sagittal plane with respect to the angle of the tibia to gravity. The model is built solving a third order polynomial regression on multiple stance phase position data sets with measurement of x- and y positions of the radar sensor with respect to the tibia angle as shown in Fig. 4.

$$\begin{pmatrix} x_w \\ y_w \end{pmatrix} = f(\phi) = A_1\phi^3 + A_2\phi^2 + A_3\phi + A_4 \tag{5}$$

The tibia angle is estimated using a gradient descent algorithm presented in [17] which is a robust implementation for angle estimation.

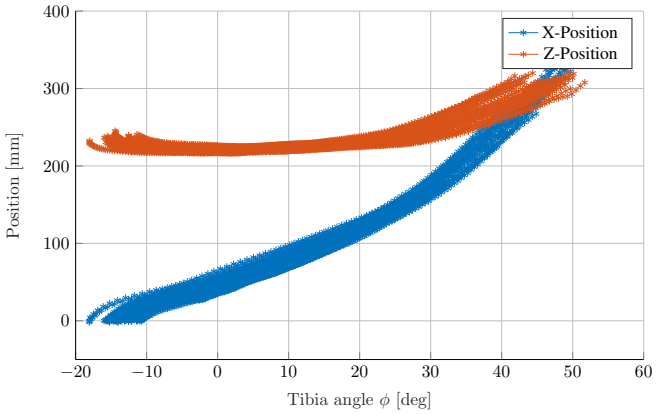

Fig. 4. Trajectory of a point on the tibia section in sagittal plane from 36 stance phases

TABLE II
TABLE OF INTRODUCTORY EVENT AND CORRESPONDING GAIT PHASES

State	Gait Phase	Event
0	Swing Phase	Toe Off
1	Stance Phase 1	Initial Contact
2	Stance Phase 2	Heal Off

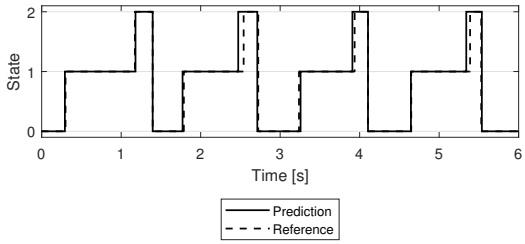

Fig. 5. Evaluation with test data of four gait samples

B. Gait phase detection using neural networks

The aim is to develop an algorithm to detect the events Initial Contact (IC), Heel Off (HO) and Toe Off (TO). Similar to support vector machines, decision trees and k-nearest neighbors, neural networks are used for classification in gait analysis [18][19][20][21]. A neural network was used for event classification and a state machine for producing corresponding gait phases. For classification, a four layer neural network with 20 perceptrons in each hidden-layer was trained. Data sets consist of signals from accelerometers and gyroscopes (6 degrees of freedom) with a sampling rate of 250 frames per second. An algorithm splits the data set in multiple step windows, each with a length of 20 frames. With a sliding window of 1 frame an overlap of 19 frames occurs. For training process the events were expanded from 1 frame to 20 frames to the future. For each step window (6 x 20 data) an algorithm produced mean value (6 x 1 data), norm of the mean acceleration (1 data) and standard derivation (6 x 1 data) as input data for the neural network. Training data (31 steps) and test data (12 steps) were produced by manually marked data sets. This marked events IC, HO and TO correspond to events from [22]. This neural network is able to classify Toe Off, Initial Contact and Heal Off. A state machine switches between corresponding gait phases, depending on the classified events. (Table II). Fig. 5 shows predicted and reference states with an overlap of more than 90 %. Delay of predicted events to reference ones is shown in Fig. 6 and could cause an error in the position estimation ion in (5). This model is only valid for the motion behavior during the stance phase. The position error will not be accumulated and would affect mapping of radar distances in the beginning and end of the stance phase which is less critical for the presented approach.

V. 2D RADAR SCANNING AND CLUSTERING

A. 2D Radar Scanning during stance phase

All distance measurements during the stance phase are transformed into the global coordinate system. The outcome is a two-dimensional scanning of the structure in sagittal plane. Fig. 7 shows the scanning of a single stair with a height of 11 cm using the measured tibia angle.

B. Filtering and Clustering

A Cell-Averaging CA-CFAR algorithm [23] is applied to filter clutter noise out of the radar scan and to keep the relevant reflections. Every reflection signal below the CFAR threshold will be removed from the 2D radar scan. Reflections of objects in a radar scan appear mostly as ellipse shaped regions due to the signal shape of an echo represented in a Fourier transformed mid-frequency f_z. All reflections are clustered to continuous ellipses using the method on [24] which has been proven suitable for binary images. It provides information on the parameters of the ellipses that approximate the clustered shape. Therefore, the 2D radar scan will be converted into a binary image and clustered accordingly. The resulting area is shown in Fig. 8 and represents completely the reflection area of the stair. The distribution of the maximum back-scattered power with respect to the tibia angle as shown in Fig. 8) shows significant fluctuations due to interference effects at this wavelength. The good visibility of the object over a wide range of scanning angles is reasonable due to the fact that the stair on the ground has a dihedral corner reflector geometry which is one of the best reflectors for radar signals. The waves are reflected twice on the same objects. The relatively flat scanning angle reduces the retro reflection effect of the corner geometry.

C. Distance Measurement

The distance measurement to the clustered object is in relation to the IC event, which defines the origin of the world local coordinate system during the stance phase. A complete stance phase is necessary to scan and detect an object in front of the prosthesis and with this multiple distances are measured due to the forward motion. Therefore an analysis of the mapped object is necessary. An approximation is

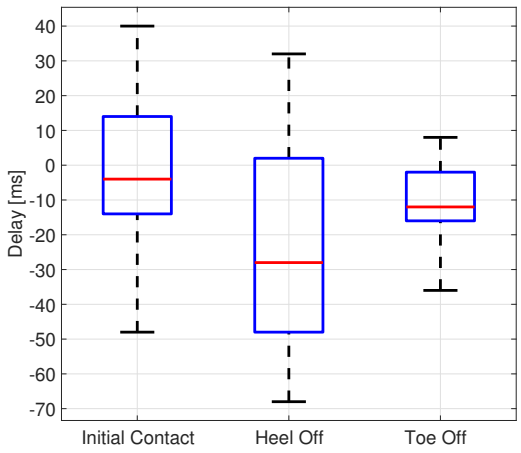

Fig. 6. Delay between predicted events to reference events of the test data, consisting of 12 gait cycles

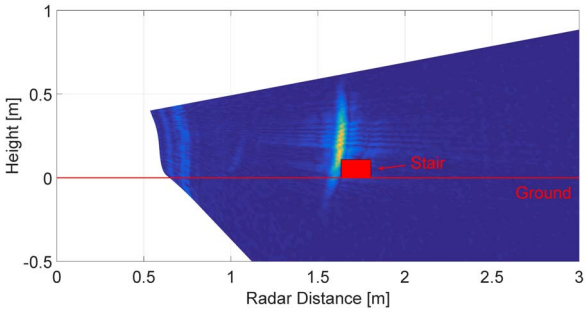

Fig. 7. 2D radar scan of an stair with height of 11 cm

the usage of the geometrical mid-point of the ellipse and has been experimental proven to be adequate for distance measurements. An experiment with a staircase conducting 33 radar scans has shown a mean distance accuracy of 1.1 ± 0.9 cm.

D. Stair Height Estimation

In comparison to laser, radar distance measurement provide information of the radial distance. This means that position of the reflection can be estimated on an radius with the measured distance R. The size of the reflection pattern is variant to the size , geometry, incident angle of the radar signal, material and surface roughness of the object. The first three parameters are the dominant ones if we assume that stairs are not made of radar absorbing materials. The approach for estimating the stair height is based on the knowledge of -3 dB area of the radar beam with an opening angle α. With (6) and starting with the tibia angle at which the clustered area first appears a for loop searches for $Q(\phi_{3\ \mathrm{dB}}) \approx -3$ dB. P_{max} is empirically determined.

$$Q(\phi) = 10 \lg \frac{P(\phi)}{P_{max}} \mathrm{dB} \tag{6}$$

At $\phi_{3\ \mathrm{dB}}$ (see yellow line in Fig. 8) we assume that the stair top reflects only -3 dB of the maximum reflected energy.

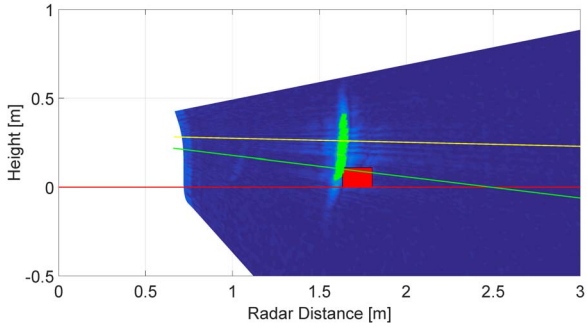

Fig. 8. Clustered 2D radar image

With $\phi_{3\ \mathrm{dB}}$ and the height h_{radar} of the radar unit in respect to ground it is possible to calculate the object height h according to (7). The green line in Fig. 8 represents the angle at $\phi_{3\mathrm{dB}} + \frac{\alpha}{2}$.

$$h = h_{radar} - sin(\phi_{3\mathrm{dB}} + \frac{\alpha}{2})R \tag{7}$$

VI. RESULTS

The presented approach has the capability to detect stairs of different heights and distances. Figure 9 shows an overlay of different radar scan of the same stair at different distances. All stairs can be clustered and detected as single objects with a certain height. For stair distance measurement, the

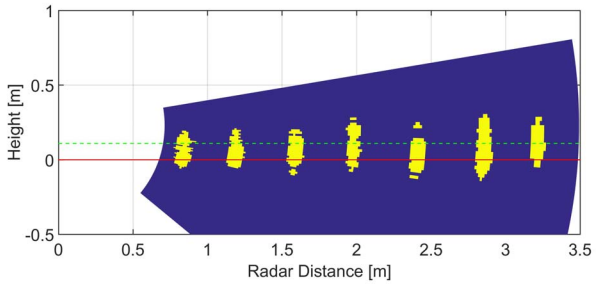

Fig. 9. Overlay of 7 stairs scans with a height of 11cm at different distances. The red line represents the ground. The green line marks the height of the measured stair.

used method provided a mean accuracy of 1.5 $\pm$0.8 cm for a range up to 5 m. Different stair heights were estimated in a laboratory setup using a robot manipulator to simulate the prosthesis motion. Measurements of two consecutive stairs (see Fig. 10) with a height of 34.4 cm and 51.6 cm were conducted. A mean accuracy for height measurement of 0.34 $\pm$ 0.67 cm could be achieved using the proposed algorithm.

VII. CONCLUSION AND FUTURE WORK

The presented approach has its novelty in the usage of radar scanning for prosthetic application to provide terrain information to further control strategies. The inertial motion estimation in combination with a focused radar distance sensor offers new capabilities in combination with EMG or inertial based user intention recognition to provide better

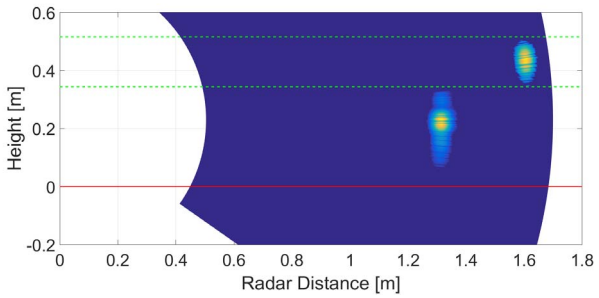

Fig. 10. A radar scan of two consecutive stairs. Only the clustered area cropped to the 3 dB level is shown. The green dashed lines mark the height of the stairs at 0.34 cm and 0.51 cm. The red line represents the ground.

quantified transition adaptions parameters for torques and angles. The results have proven that the proposed methods are valid in controlled scenarios with flat incident angles to objects and must be proven in realistic scenarios and outdoor conditions. Further studies are currently in progress:

- Distinguish between different object types using learning techniques and radar cross section (RCS) simulation models
- Investigate stair height estimation with RCS modeling and parameter variation
- Apply the approach to stair cases and slopes (ascending and descending).
- Evaluate the measurement limits for stair height estimation.

REFERENCES

[1] Jimenez-Fabian, R. Verlinden, O.: Review of control algorithms for robotic ankle systems in lower-limb orthoses, prostheses, and exoskeletons. In: Medical Engineering & Physics 34 (2012), Nr. 4, pp. 397-408.

[2] R. M. Stolyarov, G. Burnett and H. Herr, "Translational Motion Tracking of Leg Joints for Enhanced Prediction of Walking Tasks," in IEEE Transactions on Biomedical Engineering, vol. PP, no. 99, pp. 1-1.

[3] O. A. Kannape and H. M. Herr, Volitional control of ankle plantar flexion in a powered transtibial prosthesis during stair-ambulation, 2014 36th Annual International Conference of the IEEE Engineering in Medicine and Biology Society, Chicago, IL, 2014, pp. 1662-1665.

[4] Kebin Yuan, Qining Wang, Jinying Zhu, Long Wang, A Hierarchical Control Scheme for Smooth Transitions between Level Ground and Ramps with a Robotic Transtibial Prosthesis, IFAC Proceedings Volumes, Volume 47, Issue 3, 2014.

[5] B. Kleiner, Robust terrain detection system for the predictive control of active terrainadaptive limb prostheses, 13th ISPO World Congress, 2010

[6] B.Kleiner, Laser and radar based terrain recognition enables comfort and safety for stair walking with active lower limb prosthesis, ISPO World Congress, 2015

[7] S. Abdulatif, B. Kleiner, F. Aziz, C. Riehs, R. Cooper and U. Schneider, Stairs detection for enhancing wheelchair capabilities based on radar sensors, 2017 IEEE 6th Global Conference on Consumer Electronics (GCCE), Nagoya, 2017, pp. 1-5.

[8] Rouse, Elliott J.; Villagaray-Carski, Nathan C.; Emerson, Robert W.; Herr, Hugh M. (2015): Design and Testing of a Bionic Dancing Prosthesis. In: PloS one 10 (8)

[9] Dadashi F, Mariani B, Rochat S, Buela CJ, Santos-Eggimann B, Aminian K. Gait and Foot Clearance Parameters Obtained Using Shoe-Worn Inertial Sensors in a Large-Population Sample of Older Adults. Sensors (Basel, Switzerland). 2014;14(1):443-457.

[10] Riener, Robert, et al (2002): Stair ascent and descent at different inclinations, Gait & Posture, vol. 15, no. 1, 2002, pp. 3244.

[11] C. Zech et al., A compact W-band LFMCW radar module with high accuracy and integrated signal processing, 2015 European Microwave Conference (EuMC), Paris, 2015, pp. 554-557.

[12] Kleiner, Bernhard; Munkelt, Christoph; Thorhallsson, Torfi; Notni, Gunther; Kuehmstedt, Peter; Schneider, Urs (2014): Handheld 3D Scanning with Automatic Multi-View Registration Based on Visual-Inertial Navigation. In: International Journal of Optomechatronics.

[13] IEEE Standard for Safety Levels with Respect to Human Exposure to Radio Frequency Electromagnetic Fields, 3 kHz to 300 GHz

[14] Guidelines for limiting exposure to time-varying electric, magnetic, and electromagnetic fields (up to 300 GHz). International Commission on Non-Ionizing Radiation Protection. Health Phys. 1998 Apr;74(4):494-522. Review. Erratum in: Health Phys 1998 Oct;75(4):442.

[15] Filippeschi, Alessandro; Schmitz, Norbert; Miezal, Markus; Bleser, Gabriele; Ruffaldi, Emanuele; Stricker, Didier (2017): Survey of Motion Tracking Methods Based on Inertial Sensors. A Focus on Upper Limb Human Motion. In: Sensors (Basel, Switzerland) 17 (6).

[16] Hansen, A. H.; Childress, D. S. (2000): Roll-over shapes of the human foot/ankle complex. In: Engineering in Medicine and Biology Society, 2000. Proceedings of the 22nd Annual International Conference of the IEEE, Bd. 2, S. 828-830.

[17] S. O. H. Madgwick, A. J. L. Harrison and R. Vaidyanathan, "Estimation of IMU and MARG orientation using a gradient descent algorithm," 2011 IEEE International Conference on Rehabilitation Robotics, Zurich, 2011, pp. 1-7.

[18] Sepulveda, F.; Wells D. M.; Vaughan C. L.: A Neural Network Representation of Electromyography and Joint Dynamics in Human Gait, Journal of Biomechanics 2 (1993), Nr. 26, S. 101-109

[19] Shirsath, Vaishali Bhausaheb; Dongare, M. P.(2016): Neural network based gait phases of above knee prosthesis. In: 2016 IEEE International Conference on Advances in Electronics, Communication and Computer Technology (ICAECCT), 2016, Pune, India, S. 55-59

[20] Tileyliolu, E.; Yilmaz, A. (2015): Application of neural based estimation algorithm for gait phases of above knee prosthesis. In: Annual International Conference of the IEEE Engineering in Medicine and Biology Society. IEEE Engineering in Medicine and Biology Society. Annual Conference 2015, S. 4820-4823.

[21] Altinoz, O. Tolga; Yilmaz, Atila (2010): Prediction of knee angle from accelerometer data for microcontroller implementation of semi-active knee prosthesis. In: 2010 15th National Biomedical Engineering Meeting, Antalya, S. 1-4 Annual Conference 2015, S. 4820-4823.

[22] Perry, J.: Gait analysis: Normal and pathological function, Thorofare, NJ: Slack, 1992

[23] Richards, M. A. Fundamentals of Radar Signal Processing. New York: McGraw-Hill, 2005.

[24] C. Panagiotakis and A. Argyros, Parameter-free Modelling of 2D Shapes with Ellipses, Pattern Recognition, 2015.